ACS Catalysis

Research Article

pubs.acs.org/acscatalysis

Water Oxidation Catalysis Beginning with $Co_4(H_2O)_2(PW_9O_{34})_2^{10-}$ When Driven by the Chemical Oxidant Ruthenium(III)tris(2,2′-bipyridine): Stoichiometry, Kinetic, and Mechanistic Studies en Route to Identifying the True Catalyst

Jordan J. Stracke and Richard G. Finke*

Chemistry Department, Colorado State University, Fort Collins, Colorado 80523, United States

Supporting Information

ABSTRACT: Stoichiometry and kinetics are reported for catalytic water oxidation to O_2 beginning with the cobalt polyoxometalate $Co_4(H_2O)_2(PW_9O_{34})_2^{10-}$ (Co_4POM) and the chemical oxidant ruthenium(III)tris(2,2′-bipyridine) ($Ru(III)(bpy)_3^{3+}$). This specific water oxidation system was first reported in a 2010 *Science* paper (Yin et al. *Science* **2010**, *328*, 342). Under standard conditions employed herein of 1.0 μM Co_4POM, 500 μM $Ru(III)(bpy)_3^{3+}$, 100 μM $Ru(II)(bpy)_3^{2+}$, pH 7.2, and 0.03 M sodium phosphate buffer, the highest O_2 yields of 22% observed herein are seen when $Ru(II)(bpy)_3^{2+}$ is added prior to the $Ru(III)(bpy)_3^{3+}$ oxidant; hence, those conditions are employed in the present study. Measurement of the initial O_2 evolution and $Ru(III)(bpy)_3^{3+}$ reduction rates while varying the initial pH, $[Ru(III)(bpy)_3^{3+}]$, $[Ru(II)(bpy)_3^{2+}]$, and $[Co_4POM]$ indicate that the reaction follows the empirical rate law: $-d[Ru(III)(bpy)_3^{3+}]/dt = (k_1 + k_2)[Co_4POM]_{soluble}[Ru(III)(bpy)_3^{3+}]/[H^+]$, where the rate constants $k_1 \sim 0.0014\ s^{-1}$ and $k_2 \sim 0.0044\ s^{-1}$ correspond to the water oxidation and ligand oxidation reactions, and for O_2 evolution, $d[O_2]/dt = (k_1/4)[Co_4POM]_{soluble}[Ru(III)(bpy)_3^{3+}]/[H^+]$. Overall, at least seven important insights result from the present studies: (i) Parallel WOC and $Ru(III)(bpy)_3^{3+}$ self-oxidation reactions well documented in the prior literature limit the desired WOC and selectivity to O_2 in the present system to ≤28%. (ii) The formation of a precipitate from ~2 $Ru(II)(bpy)_3^{2+}$/3 $Co_4(H_2O)_2(PW_9O_{34})_2^{10-}$ with a $K_{sp} = (8 \pm 7) \times 10^{-25}$ (M^5) greatly complicates the reaction and interpretation of the observed kinetics, but (iii) the best O_2 yields are still when $Ru(II)(bpy)_3^{2+}$ is preadded. (iv) CoO_x is 2−11 times more active than Co_4POM under the reaction conditions, but (v) Co_4POM is still the dominant WOC under the $Co_4POM/Ru(III)(bpy)_3^{3+}$ and other reaction conditions employed. The present studies also (vi) confirm that the specific conditions matter greatly in determining the true WOC and (vii) allow one to begin to construct a plausible WOC mechanism for the $Co_4POM/Ru(III)(bpy)_3^{3+}$ system.

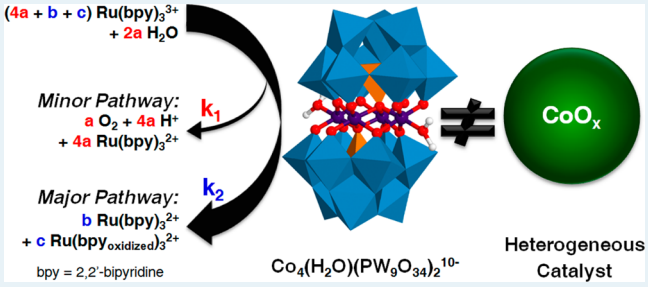

KEYWORDS: *water oxidation, kinetics and mechanism, homogeneous versus heterogeneous, polyoxometalate catalyst, ligand oxidation*

INTRODUCTION

Catalysts capable of efficiently transforming abundant materials, such as water and carbon dioxide, into fuel and oxygen are of great interest for the advancement of renewable energy storage.[1−5] Water oxidation catalysts (WOCs) with stability, selectivity, affordability, and high activity at low driving forces (i.e., low overpotentials) are critical to the implementation of the desired energy storage, solar fuels, and other technology.[4,6−13] To understand and rationally improve these WOCs, it is necessary to study the mechanism by which they oxidize water to O_2.[14,15]

Polyoxometalates are of interest as WOCs because these metal oxide compounds are discrete, contain no oxidizable organic ligands, can be synthetically altered, and can be models for heterogeneous metal oxide catalysts,[16,17] properties that make them good candidates for mechanistic water oxidation studies.[18−21] Despite these apparent advantages of POM-based WOCs, only a few studies have examined the kinetics and mechanisms of polyoxometalate WOCs.[22−26]

Co_4POM is of particular interest and, hence, the focus of the current investigation because it incorporates the moderately earth abundant element cobalt. Water oxidation catalysis by this POM was first reported by Hill and co-workers in a 2010 *Science*[27] and a 2011 *JACS* paper,[28] and subsequent studies have investigated the identity of the true water oxidation catalyst.[29−31] In the *Science* paper, ruthenium(III)tris(2,2′-bipyridine) ($Ru(III)(bpy)_3^{3+}$) was used as a chemical oxidant to drive the oxidation of water to oxygen with a reported TOF of up to 5 s^{-1} under the specific conditions of 3.2 μM Co_4POM, 1500 μM $Ru(III)(bpy)_3^{3+}$, pH 8.0, and 0.03 M sodium phosphate buffer.[27] However, the prior studies of Co_4POM

Received: August 16, 2013
Revised: November 7, 2013
Published: December 9, 2013

   dx.doi.org/10.1021/cs4006925 | *ACS Catal.* 2014, 4, 79−89

using $Ru(III)(bpy)_3^{3+}$ as an oxidant do not include kinetic studies en route to establishing the water oxidation mechanism, studies that are of importance for comparing the activity, selectivity, and stability of different catalyst species as well as for assisting in identifying the true active catalyst.[32]

As studied by Creutz and Sutin et al.[33−35] and as noted in the 2010 *Science* paper, when $Ru(III)(bpy)_3^{3+}$ is used as an oxidant, bipyridine ligand oxidation occurs in parallel with water oxidation; this results in oxygen yields that are always less than 100% and concomitant nonoptimal selectivity to O_2. Creutz and Sutin et al. also thoroughly investigated the kinetics and mechanism of both the cobalt(II)-catalyzed and uncatalyzed reduction of the $Ru(III)(bpy)_3^{3+}$ species.[33−35] That classic work showed that the uncatalyzed reduction of $Ru(III)(bpy)_3^{3+}$ into $Ru(II)(bpy)_3^{2+}$ plus oxidized bipyridine ligand products, $Ru(bpy_{ox})_3^{2+}$, is dependent on the $[Ru(III)(bpy)_3^{3+}]$ in two parallel paths that are dependent on $[OH^-]$ and $[OH^-]^2$, under their conditions of pH ≥ 12 and initial $[Ru(III)(bpy)_3^{3+}]$ of 30−170 μM.[35]

In the presence of a cobalt(II) precatalyst, Creutz and Sutin quantitated oxygen generation; they also followed $Ru(III)(bpy)_3^{3+}$ loss, which yielded the rate law[34,35]

$$-d[Ru(III)(bpy)_3^{3+}] = \frac{k_{Co}[Ru(bpy)_3^{3+}]^2[Co]}{[Ru(bpy)_3^{2+}][H^+]^2} \quad (1)$$

The combination of the water oxidation (eq 2) and ligand oxidation (eq 3) parallel pathways results in an overall

$$2a\ H_2O + 4a\ Ru(bpy)_3^{3+} \rightarrow a\ O_2 + 4a\ H^+ + 4a\ Ru(bpy)_3^{2+} \quad (2)$$

$$(b+c)\ Ru(bpy)_3^{3+} \rightarrow b\ Ru(bpy)_3^{2+} + c\ Ru(bpy_{ox})_3^{2+} \quad (3)$$

+

$$2a\ H_2O + (4a+b+c)\ Ru(bpy)_3^{3+} \rightarrow a\ O_2 + 4a\ H^+ + (4a+b)\ Ru(bpy)_3^{2+} + c\ Ru(bpy_{ox})_3^{2+} \quad (4)$$

generalized reaction stoichiometry given in eq 4, where $Ru(bpy_{ox})_3^{2+}$ encompasses all the possible products formed when a ruthenium(II)tris(bipyridine) species undergoes one or more bipyridine ligand oxidation reactions.

Although classic work of Creutz and Sutin did not identify the true active catalyst in their reactions, other studies have identified CoO_x colloids to be the active WOC when beginning with Co(II) salts and $Ru(III)(bpy)_3^{3+}$.[36−38] Styring and co-workers have also shown a correlation between decreased CoO_x colloid size and increased activity (i.e., presumably between increasing number of surface sites and, therefore, increasing activity).[36] Hence, studies that contain cobalt precursors should attempt to rule out the possibility that the starting material is transformed into a heterogeneous, colloidal CoO_x catalyst under the reaction conditions.

Prior studies have investigated this possibility of in situ CoO_x formation when beginning with Co_4POM. In electrochemical studies of Co_4POM, we found that when a glassy carbon electrode at 1.1 V vs Ag/AgCl was used as the oxidant source in 500 uM Co_4POM solutions, the dominant WOC is actually a heterogeneous CoO_x material and not the starting Co_4POM.[29] More recently, in a deliberate attempt to try to favor water oxidation catalysis by the cobalt polyoxometalate, we reported that when the Co_4POM concentration is lowered to 2.5 uM and the electrode potential is increased to >1.3 V vs Ag/AgCl—again, in an attempt to favor a discrete Co_4POM-based WOC—we were unable to distinguish between a true POM catalyst and CoO_x-based catalysis.[31] Specifically and in that study, key controls revealed that if even 8.2% of the POM was converted into CoO_x, then that amount of CoO_x catalyst would account for all of the O_2 produced during a 60s electrolysis at 1.4 V. In addition, we measured the $[Co_4POM]$ by HPLC after the electrolysis and found that 9.4 ± 5.1% of the Co_4POM was absent at the end of the electrolysis experiment. In the end, and under those conditions designed to favor a Co_4POM-based WOC, we were unable to unambiguously identify the true WOC. Those studies demonstrate the difficulty of determining the identity of the true water oxidation catalyst when the alternative heterogeneous decomposition material is extremely active, as is typically observed for CoO_x.[31]

In another study, Sartorel and Scandola used flash photolysis experiments, which indicated that neither Co^{2+} (i.e., CoO_x) or Co_4POM was the active catalyst.[30] Instead, they favored a Co_4POM decomposition product as the true WOC (i.e., a different but as yet unknown POM) when using, now, a photochemically derived Ru(III) oxidant. However, and as pointed out by Hill and co-workers,[39] Sartorel and Scandola did not quantify O_2 generation in their experiments,[30] and therefore, the precise reaction that they were studying remains unclear.

Most recently, Hill and co-workers have addressed the question of homogeneous vs heterogeneous catalysis when beginning with Co_4POM.[39] They reported precatalysis stability and dissociation to $[Co^{2+}]_{apparent,aqueous}$ measurements using cathodic stripping voltammetry, clever extraction experiments of anionic species using tetraheptylammonium nitrate, $Ru(III)(bpy)_3^{3+}$ loss measurements comparing Co_4POM and $Co(NO_3)_2$ controls, and pH variation plus O_2 quantification experiments.[39] Although an amount of CoO_x equivalent to the four cobalts in Co_4POM was shown to be the superior catalyst in terms of total turnovers or rate of O_2 formation (Table 2 of ref 39), overall, the results support the authors' previous conclusion[27] that that the observed WOC derives from Co_4POM and not heterogeneous CoO_x under the conditions studied and when $Ru(III)(bpy)_3^{3+}$ is used as the chemical oxidant. However, the precise identity of the true, active WOC was not the focus of that work so that the detailed kinetic studies and full rate law, necessary to begin to answer the challenging question of the precise identity of the true catalyst, were not reported therein[39] or previously[27,28] because, again, that was not the focus of their studies.

Herein, we report the stoichiometry and kinetics of water oxidation when beginning with Co_4POM and the $Ru(III)(bpy)_3^{3+}$ oxidant under conditions when excess $Ru(II)(bpy)_3^{2+}$ is added prior to $Ru(III)(bpy)_3^{3+}$, conditions that give the best O_2 yields, which are also relevant to literature photochemically driven oxidations which employ $Ru(II)(bpy)_3^{2+}$ and are useful in understanding the influence of the $Ru(bpy)_3^{2+}$ byproduct.[28,30,39] The Co_4POM results are then compared with those for an in situ formed CoO_x WOC to provide further insight into the true WOC when beginning with Co_4POM and $Ru(III)(bpy)_3^{3+}$. In this comparison, we find differing trends in the selectivity and activity of the Co_4POM and CoO_x, kinetic and mechanistic evidence that strongly suggests the active catalysts in these two systems are, indeed, distinguishable as Professor Hill and his co-workers have argued.[27,28,39] We also discuss, briefly, the drawbacks of the $Ru(III)(bpy)_3^{3+}$-based chemical oxidant system and what is, and is not, known about the true catalyst in both the Co_4POM and CoO_x cases. Last, we

dx.doi.org/10.1021/cs4006925 | ACS Catal. 2014, 4, 79−89

propose a water oxidation mechanism consistent with our evidence in the case of catalysis beginning with Co_4POM.

EXPERIMENTAL SECTION

Materials. $Na_{10}Co_4(H_2O)_2(PW_9O_{34})_2$ was synthesized and recrystallized according to the method of Weakley et al.[40] with modifications reported by Yin et al.[27] Its identity was verified by ^{31}P NMR, IR, and UV−vis spectroscopies, which matched published characterization data.[27] $Co(NO_3)_2$, Na_2HPO_4, and NaH_2PO_4 were obtained from Sigma-Aldrich or Fisher and used without further purification.

Ruthenium(III)tris(2,2′-bipyridine) triperchlorate (Ru(III)-$(bpy)_3^{3+}$) and ruthenium(II)tris(2,2′-bipyridine) diperchlorate were synthesized from ruthenium(II)tris(2,2′-bipyridine) dichloride according to the method of Creutz and Sutin.[34] The ruthenium(III)tris(2,2′-bipyridine)triperchlorate matched the published molar absorptivity ($\varepsilon_{675\ nm}$ = 440 $M^{-1}\cdot cm^{-1}$).[34] The ruthenium(II)tris(2,2′-bipyridine)diperchlorate was recrystallized by dissolving in a minimum amount of water at room temperature, with crystallization occurring at 5 °C over 1 day.

Clark Electrode Calibration. The Clark electrode was calibrated prior to O_2 evolution experiments using 0% and 20.9% (air) standard solutions. These values correspond to typical O_2 concentrations of 0 and 236 μM after correcting for temperature and air pressure.

O_2 Evolution and Yield Quantification. In a 1 dram vial with a stir bar, a solution was prepared using stock solutions of 0.2 M sodium phosphate buffer (pH 6.8−7.8), 0.2 mM Co_4POM (or $Co(NO_3)_2$), and 0.5 mM Ru(II)$(bpy)_3(ClO_4)_2$. A calibrated Clark electrode (Microelectrodes Inc.) was immersed in the solution. For example, a reaction run under standard conditions contained 1.1 mL of water, 0.4 mL of Ru(II)$(bpy)_3^{2+}$ stock solution, and 10 μL of Co_4POM solution. The Ru(II)$(bpy)_3^{2+}$ and Co_4POM solutions were combined 42 ± 9 s before addition of Ru(III)$(bpy)_3^{3+}$ unless otherwise specified; this aging time was needed to ensure the Clark electrode reading was stable prior to initiation of the reaction. The solution was stirred at 600 rpm. Next, a solution of Ru(III)$(bpy)_3(ClO_4)_3$ was prepared by dissolving the solid in water. For example, a 5 mM Ru(III)$(bpy)_3^{3+}$ solution was prepared by dissolving 8.68 mg of Ru(III)$(bpy)_3^{3+}$ in 2.00 mL of H_2O with sonication (∼10−30 s). The dissolved O_2 concentration was recorded before adding the Ru(III)$(bpy)_3^{3+}$ solution to the Co_4POM (or $Co(NO_3)_2$) solution via autopipette to ensure a stable baseline response of the Clark electrode. A reaction under standard conditions used 0.20 mL of the stock Ru(III)$(bpy)_3^{3+}$ solution; reactions that contained [Ru(III)$(bpy)_3^{3+}$] ≥ 0.5 mM used a stock solution of 5.0 mM Ru(III)$(bpy)_3^{3+}$, and reactions that had lower oxidant concentrations used 1.0 mM Ru(III)$(bpy)_3^{3+}$ stock solutions. Immediately after addition of the Ru(III)$(bpy)_3^{3+}$ solution, stirring was stopped, and the reaction was allowed to proceed until the electrode response plateaued, at which time stirring was resumed and the final O_2 concentration reading was taken. Reactions were typically 2−5 min in length. This procedure was followed to minimize the solution-to-gas transfer of O_2 generated during the reaction so the O_2 yield could be measured in solution.

Kinetics of O_2 Evolution. Oxygen evolution rates were measured using a custom-built Clark electrode that was made according to the method of Bard and co-workers,[41] except a 368 μm diameter platinum wire (Alfa Aesar, 99.95% purity) was used, and the reference solution contained 0.2 M NaCl plus 0.2 M, pH 8.0 sodium phosphate. This electrode has a faster response time than the commercial Microelectrodes O_2 electrode and is therefore better suited to the kinetic experiments herein (i.e., the 95% response time is ∼2−3 s going from 236 to 0 μM O_2 solution). The electrode was polarized at −800 mV and was allowed to equilibrate with the solution before starting the experiment; typical equilibration times were 3−5 min. The current was recorded every 0.1 s using a CHI630D potentiostat and software (CH Instruments Inc.).

Reactions were run using the procedure described in the "O_2 Evolution and Yield Quantification" section above, except the reaction was stirred throughout the reaction and the electrode was recalibrated at the end of each reaction. The initial O_2 evolution rate, $\{d[O_2]/dt\}_i$, was measured by linearly fitting the first 5−10 s of the electrode response, where the fitted slope corresponds to the initial rate. See Supporting Information Figure S1 for sample data.

Kinetics of Ru(III)$(bpy)_3^{3+}$ Loss. The water oxidation reaction was run as described in the "O_2 Evolution and Yield Quantification" section with the following alterations: (1) the reaction was run in a plastic cuvette (Spectronic, 1 cm path length) and (2) the reaction was not stirred during the reaction, but was mixed when the reactants were combined by quickly removing and reinjecting a portion of the solution using an autopipette. The concentration of Ru(III)$(bpy)_3^{3+}$ was monitored by the absorbance at 675 nm using the known molar absorptivity, $\varepsilon_{675\ nm}$ = 440 $M^{-1}\cdot cm^{-1}$. Data points were collected every 1.0 s for 60 s on an HP 8452A diode array spectrometer. The initial ruthenium(III) reduction rate, $\{-d[Ru(III)(bpy)_3^{3+}]/dt\}_i$, was measured by linearly fitting the first ∼10% of the reaction (i.e., typically the first 5−10 s of the reaction). Sample data are given in Supporting Information Figure S1.

K_{sp} Measurement of the Co_4POM−Ru(II)$(bpy)_3$ Precipitate. Four solutions were prepared in 0.03 M, pH 7.2 sodium phosphate buffer and contained 100 μM Ru(II)$(bpy)_3^{2+}$ plus 0, 5.0, 10.0, or 20.0 μM Co_4POM. After 8 h, the solutions were filtered through 0.22 μm nylon syringe filters into plastic cuvettes, and the absorbance spectra were recorded and analyzed to determine the equivalents of Ru(II)$(bpy)_3^{2+}$ per Co_4POM in the precipitate (found ∼2:3 Co_4POM/Ru(II)-$(bpy)_3^{2+}$). Three solutions were prepared in 0.03 M, pH 7.2 sodium phosphate buffer containing the Co_4POM and Ru(II)$(bpy)_3^{2+}$ in the predetermined 1:1.5 ratio: (1) 10.0:15.0 μM; (2) 20.0:30.0 μM; (3) 50.0:75.0 μM. After 8 h, these solutions were filtered through 0.22 μm nylon syringe filters, and the absorbance spectra were measured to determine the remaining [Ru(II)$(bpy)_3^{2+}$], which was used to calculate the K_{sp} value.

RESULTS AND DISCUSSION

Stoichiometry of the Oxidation Reaction. As discussed in the Introduction, the catalytic oxidation of water into oxygen using the terminal oxidant Ru(III)$(bpy)_3^{3+}$ nearly always results in substoichiometric production of O_2 because of the parallel oxidation of the 2,2′-bipyridine ligands. The net observed stoichiometry and selectivity of these reactions (eq 4) is therefore a measurement of the relative activity of the water oxidation reaction vs ligand oxidation. That is, the ratio of ligand versus water oxidation is a measure of the net relative production of these two parallel pathways.

dx.doi.org/10.1021/cs4006925 | ACS Catal. 2014, 4, 79−89

We therefore began our investigation of the Co_4POM by determining the stoichiometry of the POM-catalyzed water oxidation reaction. Throughout the current investigation, a standard reaction is run by making a solution of the Co_4POM in 0.30 M sodium phosphate buffer, adding a 0.50 mM $Ru(II)(bpy)_3^{2+}$ solution (except in controls or other experiments, where it was intentionally omitted), and then adding a $Ru(III)(bpy)_3^{3+}$ solution to initiate the reaction. The dissolved oxygen concentration was then measured using a Clark electrode immersed in the reaction solution.

The O_2 yields for a series of experiments are shown in Table 1. The data reveal several interesting insights, including (i) the

Table 1. O_2 Yields for $Ru(III)(bpy)_3^{3+}$ Plus Co_4POM Reactions[a]

entry	[Co_4POM] (μM)	[Ru(III)] (μM)	[Ru(II)] (μM)	pH	O_2 yield (μM)	% yield
1	0.5	100	100	7.2	5	20
2	1.0	100	100	7.2	3	12
3	2.0	100	100	7.2	4	16
4	1.0	50	100	7.2	1	8
5	1.0	200	100	7.2	9	18
6	1.0	500	100	7.2	27	22
7	1.0	750	100	7.2	40	21
8	1.0	1000	100	7.2	47	19
9	1.0	500	50	7.2	26	21
10	1.0	500	200	7.2	12	10
11	1.0	500	100	6.8	8	6
12	1.0	500	100	7.5	31	25
13	1.0	500	100	7.8	35	28
14[b]	1.0	500	100	7.2	9	7
15[b]	1.0	1000	100	7.2	20	8
16	1.0	500	0	7.2	13	10
17	0	500	100	7.2	2	2

[a]The order of experiments in this table is organized by listing entries in sets that vary the concentration of [POM] (entries 1–3), [$Ru(III)(bpy)_3^{3+}$] (4–8), [$Ru(II)(bpy)_3^{2+}$] (9–10), and pH (11–13). [b]$Ru(III)(bpy)_3^{3+}$ and $Ru(II)(bpy)_3^{2+}$ were added simultaneously; for all other experiments, $Ru(II)(bpy)_3^{2+}$ was combined with the Co_4POM solution 42 ± 9 s before addition of the $Ru(III)(bpy)_3^{3+}$.

O_2 yields are considerably higher when $Ru(II)(bpy)_3^{2+}$ is added prior to $Ru(III)(bpy)_3^{3+}$ (entries 6 and 8 versus 14 and 15); (ii) the ligand oxidation path is always favored by at least 3-fold under the various conditions examined herein; and (iii) the O_2 yields increase with increasing pH (entries 6, 11–13) and increasing [$Ru(III)(bpy)_3^{3+}$] (entries 4–8). These results indicate the active catalyst(s) in Co_4POM solutions show poor selectivity for water oxidation relative to ligand oxidation.

Kinetics of O_2 Formation. Kinetics of oxygen evolution were measured directly by a Clark electrode to gain further insight into the water oxidation mechanism. Since addition of $Ru(II)(bpy)_3^{2+}$ to the Co_4POM solution yields larger amounts of O_2, all kinetic experiments include preadded $Ru(II)(bpy)_3^{2+}$. The O_2 evolution rates displayed a complex dependence on the Co_4POM, $Ru(III)(bpy)_3^{3+}$, $Ru(II)(bpy)_3^{2+}$, and H^+ concentrations. Therefore, the method of initial rates was used to derive an empirical rate law for the Co_4POM precatalyst.

Figure 1 shows the initial rate data for O_2 evolution with variation in the initial concentration for each of [Co_4POM], [$Ru(III)(bpy)_3^{3+}$], [$Ru(II)(bpy)_3^{2+}$], and [H^+] while holding the other three concentrations constant. Note that for all initial rate data ($\{d[O_2]/dt\}_i$ and $\{d[Ru(III)(bpy)_3^{3+}]/dt\}_i$), the given concentrations and pH values are the initial conditions for the reaction. When using a Co_4POM precatalyst, these initial rate plots are consistent with a first-order dependence on the [$Ru(III)(bpy)_3^{3+}$] oxidant and inverse-first-order dependences on [$Ru(II)(bpy)_3^{2+}$] and [H^+]. The fits to other reaction orders are less satisfactory (Supporting Information Table S1 and S2).

Interestingly, Figure 1C reveals only a small dependence of the initial O_2 evolution rate on the initial Co_4POM concentration, suggesting that the actual water oxidation catalyst concentration changes little between these experiments. Indeed, this curve is fit well by either first-to-zero-order saturation kinetics or a 0.25-order fit (although the latter makes little physical sense). This observation suggests two possible hypotheses: (i) precipitation of a $Ru(II)(bpy)_3^{2+}$–Co_4POM^{10-} complex, in which only a relatively constant amount of Co_4POM remains in solution, or (ii) decomposition of the Co_4POM into a different, possibly heterogeneous, catalyst in which the number of active sites does not scale linearly with the precursor concentration.

Evidence for a Precipitate Formed With a ~2:3 $Co_4POM/Ru(II)(bpy)_3^{2+}$ Ratio, Its K_{sp} and Its Effect on the Kinetics. To investigate this substoichiometric precatalyst dependence phenomenon further, the Co_4POM plus $Ru(II)(bpy)_3^{2+}$ solution was aged prior to addition of $Ru(III)(bpy)_3^{3+}$. Consistent with the precipitation hypothesis, the initial O_2 evolution rate decreases from 0.34 to 0.22 to 0.12 μM/s for 30, 60, or 120 s aging times (Supporting Information Figure S2). In addition, when Co_4POM is combined with $Ru(II)(bpy)_3^{2+}$, a precipitate forms in a ~2:3 $Co_4POM/Ru(II)(bpy)_3^{2+}$ ratio, and this precipitate has a $K_{sp} = (8 \pm 7) \times 10^{-25}$ (M^5) (Supporting InformationTables S3 and S4). These observations are in-line with precedents for ion-pairing and aggregation between $Ru(II)(bpy)_3^{2+}$ and polyoxometalates. Specifically, $[Ru_4O_4(\mu\text{-}OH)_2(H_2O)_4(\gamma\text{-}SiW_{10}O_{36})_2]^{10-}$, $[PW_{12}O_{40}]^{3-}$, and $[PW_{11}O_{39}]^{7-}$ have been reported to form POM/$Ru(II)(bpy)_3^{2+}$ complexes in ~1:4,[26] 1:1,[42] and 1:1[42] ratios. This literature precedent and low observed K_{sp} value observed herein demonstrate the importance of considering $Co_4(H_2O)_2(PW_9O_{34})_2^{10-}$/$Ru(II)(bpy)_3^{2+}$ solution/precipitate equilibria in the study of O_2 evolution kinetics of highly negatively charged polyoxometalates.

Because addition of Ru(II) to the Co_4POM solution appears to induce precipitation, we next addressed whether the inverse, $[Ru(II)(bpy)_3^{2+}]^{-1}$ dependence in Figure 1C, derives from precipitation (i.e., from the removal of the POM from the catalytic cycle) or from a reversible electron-transfer step within the catalytic cycle. Comparison of $\{d[O_2]/dt\}_i$ when $Ru(II)(bpy)_3^{2+}$ is added at the same time as $Ru(III)(bpy)_3^{3+}$ or when no $Ru(II)(bpy)_3^{2+}$ is added, reveals no significant difference in the initial rates ($\{d[O_2]/dt\}_i$ = 2.5 and 2.3 μM/s, respectively); that is, the initial O_2 evolution rate does not depend on the initial [$Ru(II)(bpy)_3^{2+}$] when it is added at the same time as $Ru(III)(bpy)_3^{3+}$. This strongly suggests that the inverse, $[Ru(II)(bpy)_3^{2+}]^{-1}$, dependence observed in Figure 1C is the result of the Co_4POM interacting with the $Ru(II)(bpy)_3^{2+}$ in a precipitation reaction prior to addition of oxidant. That is, the catalytically available $[Co_4POM]_{soluble}$ in the reaction is less than the initially added $[Co_4POM]_{total}$. Overall, these order-of-addition experiments, the Co_4POM plus $Ru(II)(bpy)_3^{2+}$ aging tests, and the K_{sp} determination all strongly suggest precipitation plays a significant, complicating role in the O_2 evolution reaction, the observed kinetics, and the underlying mechanism for polyoxometalate/$Ru(III)(bpy)_3^{3+}$ systems.

dx.doi.org/10.1021/cs4006925 | ACS Catal. 2014, 4, 79–89

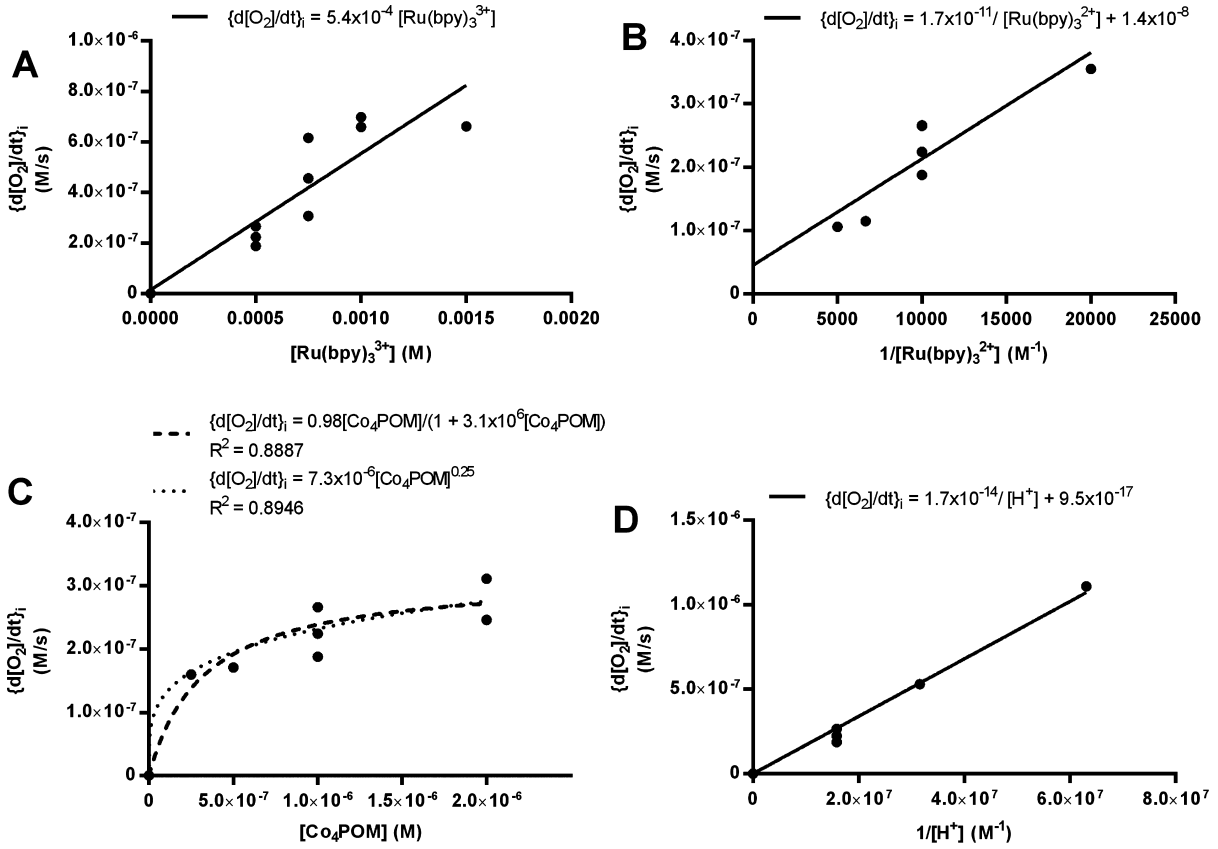

Figure 1. Initial O_2 evolution rate data measured by a custom-built Clark electrode[41] with variation in the initially added (A) $[Ru(III)(bpy)_3^{3+}]$, (B) $[Ru(II)(bpy)_3^{2+}]$, (C) $[Co_4POM]$, and (D) pH. For each of the plots, all other initial, added concentrations were held constant; the standard conditions are 1.0 μM Co_4POM, 500 μM $Ru(III)(bpy)_3^{3+}$, 100 μM $Ru(II)(bpy)_3^{2+}$, pH 7.2, and 0.03 M sodium phosphate buffer. Solid lines are linear fits. The dotted line is fit assuming a reaction order of 0.25 ($Y = aX^{0.25} + b$, where a and b are fitting parameters). Since the 0.25-order fit to the Co_4POM data (C) is physically unreasonable, plot C was also fit to a first-order reaction with saturation kinetics (dashed line) ($Y = aX/(1 + bX)$ where a and b are fitting parameters). The Y intercept for all plots was constrained to values ≥ 0. R^2 values and fits to other reaction orders can be found in the Supporting Information.

Kinetics of $Ru(III)(bpy)_3^{3+}$ Oxidant Loss. The kinetics of $Ru(III)(bpy)_3^{3+}$ loss were investigated next to extract the ligand oxidation kinetics and to allow comparison of the relative rates of the water and ligand oxidation reactions. Specifically, the oxidation of the bipyridine ligand was studied in greater detail by measuring the decrease in the 675 nm absorbance band of $Ru(III)(bpy)_3^{3+}$ while in the presence of Co_4POM. As before, the dependence of the initial rate, $\{-d[Ru(III)(bpy)_3^{3+}]/dt\}_i$, was measured while varying the initial reaction parameters; for these experiments, the initial concentrations of $[Ru(III)(bpy)_3^{3+}]$, $[Ru(II)(bpy)_3^{2+}]$, $[Co_4POM]$, and $[H^+]$ were each changed while keeping the other three initial variables constant. The obtained initial rates were then corrected by subtracting the initial $Ru(III)(bpy)_3^{3+}$ loss due to water oxidation (using the data fits in Figure 1) so that the resultant corrected rates, $\{-d[Ru(III)(bpy)_3^{3+}]_{ligand\ ox.}/dt\}_i$, reflect only the ligand oxidation path:

$$\left\{\frac{-d[Ru(bpy)_3^{3+}]_{ligand\ ox}}{dt}\right\}_i = \left\{\frac{-d[Ru(bpy)_3^{3+}]_{total}}{dt}\right\}_i - 4\left\{\frac{d[O_2]}{dt}\right\}_i \quad (5)$$

Plotting this ligand-oxidation-only initial rate data shows a first-order dependence on $[Ru(III)(bpy)_3^{3+}]$; an inverse-first-order dependence on $[Ru(II)(bpy)_3^{2+}]$ with a nonzero intercept; and an initial inverse-first-order dependence on $[H^+]$, which then flattens some at increasing pH values (Figure 2). The kinetic data also reveal an initial first-order dependence in $[Co_4POM]$ with flattening toward a lower-order dependence at increasing concentrations. Other tested fits to the data proved inferior and are provided in Supporting Information Tables S2 and S3.

The nonzero intercepts for both the Co_4POM and $Ru(II)(bpy)_3^{2+}$ plots are consistent with a background reaction of $Ru(III)(bpy)_3^{3+}$ undergoing an uncatalyzed ligand-oxidation reaction with itself (i.e., a self-oxidation), a process that has precedent in the previously cited, classic studies by Creutz and Sutin et al.[33,34] Indeed, the data in Figure 2B can be corrected by subtracting the background, uncatalyzed ligand-oxidation rate in Supporting Information Figure S3A; the 90% confidence interval for the corrected intercept is -6.9×10^{-7} to 1.7×10^{-6} (Supporting Information Figure S3B), which is within experimental error of zero.

The $1/[H^+]$ saturation kinetics are interesting because they imply either a reversible proton-transfer prior to the turnover limiting step in the reaction or that the rate changes with the concentration of the base (e.g., the $[HPO_4^{2-}]$ increases with the pH over this range). Interestingly, a similar flattening of the $1/[H^+]$ kinetics is not observed in the O_2 evolution kinetics (Figure 1D). It is unclear at present whether this modest difference in the pH dependence of the water and ligand-

dx.doi.org/10.1021/cs4006925 | ACS Catal. 2014, 4, 79−89

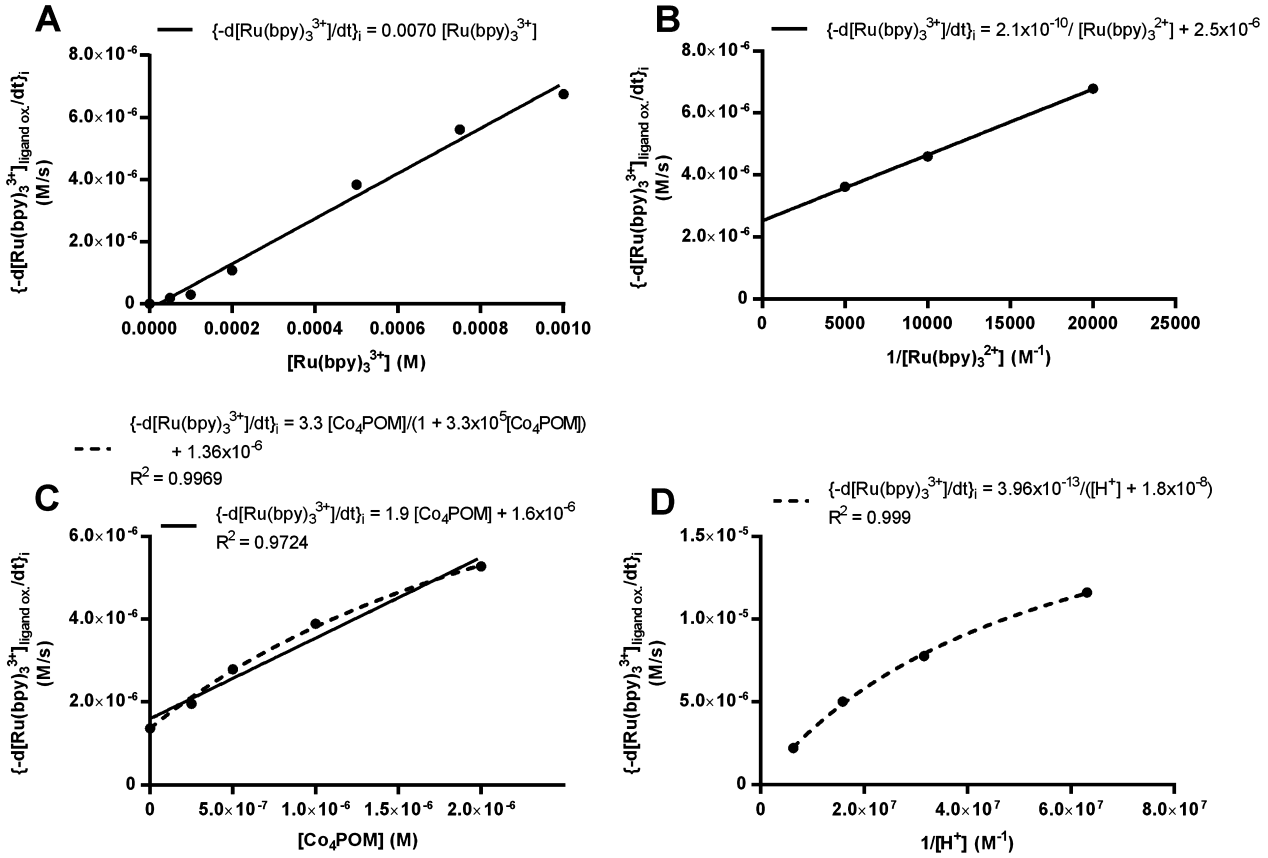

Figure 2. Initial bipyridine ligand oxidation rate data with variation in the initially added (A) $[Ru(III)(bpy)_3^{3+}]$, (B) $[Ru(II)(bpy)_3^{2+}]$, (C) $[Co_4POM]$, and (D) pH. For each of the plots, all other initial concentrations were held constant where the Standard Conditions are 1.0 μM Co_4POM, 500 μM $Ru(III)(bpy)_3^{3+}$, 100 μM $Ru(II)(bpy)_3^{2+}$, pH 7.2, and 0.03 M sodium phosphate buffer. The $\{-d[Ru(III)(bpy)_3^{3+}]/dt\}_i$ is derived from the loss in absorbance at 675 nm and after correcting for the amount of $Ru(III)(bpy)_3^{3+}$ which corresponds to O_2 evolution, as shown in eq 5. Solid lines indicate linear fits. Dashed lines are fits assuming a first-order reaction with saturation kinetics: $Y = aX/(1 + bX)$ + intercept, where a and b are fitting parameters and the intercept was set to zero for plot (C) and set to the experimentally measured intercept of 1.36×10^{-6} for plot (D). The y intercept for all plots was constrained to values ≥ 0 for all other plots. R^2 values and fits to other reaction orders can be found in the Supporting Information.

oxidation kinetics is real or due to experimental error in the O_2 kinetic measurements.

An additional complicating factor when interpreting the kinetics, as discussed in the O_2 evolution kinetics section above, concerns the origin of the observed inverse $Ru(II)(bpy)_3^{2+}$ dependence. Specifically, is the only role of $Ru(II)(bpy)_3^{2+}$ to bind/precipitate the Co_4POM^{10-} polyanion, thereby removing the Co_4POM polyoxometalate from the catalytic cycle, or is it perhaps involved as a product of a reversible $Ru(III)(bpy)_3^{3+}$-to-$Ru(II)(bpy)_3^{2+}$ electron-transfer reaction within the catalytic cycle? Consistent with the O_2 evolution kinetics, the $\{-d[Ru(III)(bpy)_3^{3+}]/dt\}$ is the same (42 and 41 μM/s) when 1.0 uM Co_4POM is combined with either 500 μM $Ru(III)(bpy)_3^{3+}$ or 500 μM $Ru(III)(bpy)_3^{3+}$ plus 100 μM $Ru(II)(bpy)_3^{2+}$ (where the $Ru(II)(bpy)_3^{2+}$ is added at the same time as the $Ru(III)(bpy)^{3+}$) in 0.03 M, pH 7.2 sodium phosphate buffer. This result suggests both the inverse $Ru(II)(bpy)_3^{2+}$ and the slight flattening of the $[Co_4POM]$ vs $\{-d[Ru(III)(bpy)_3^{3+}]_{ligand\ ox.}/dt\}_i$ curve are due primarily to the precipitation reaction between the Co_4POM and the $Ru(II)(bpy)_3^{2+}$, thereby removing Co_4POM from the catalytic cycle (i.e., the catalytically available $[Co_4POM]_{soluble}$ is less than the initially added $[Co_4POM]_{total}$) . Importantly, given that we have shown that $Ru(II)(bpy)_3^{2+}$ can precipitate the Co_4POM^{10-}, an added implication here from the above control, as well as from simple chemical intuition, is the suggestion that $Ru(III)(bpy)_3^{3+}$ might also form an ion pair with or precipitate Co_4POM^{10-}. This will be important later when interpreting the rate law for O_2 formation. But first, studies aimed at providing evidence for or against a heterogeneous CoO_x colloidal catalyst need to be presented.

Stoichiometric and Kinetic Contrasts of Co_4POM and $Co(NO_3)_2$ WOC Precursors. One recurring question when beginning with homogeneous water oxidation catalysts is whether the starting material is the true catalyst or whether the initially homogeneous complex is transformed into a heterogeneous catalyst under the reaction conditions.[43,44] To provide independent, kinetics-based evidence for the nature of the true catalyst above that already available,[27,28,39] we have collected data on the stoichiometry, oxygen evolution kinetics, and $Ru(III)(bpy)_3^{3+}$ reduction kinetics for a heterogeneous CoO_x type catalyst under the otherwise identical conditions used to study the Co_4POM. In these studies, $Co(NO_3)_2$ was used as the precursor for the heterogeneous CoO_x catalyst, a transformation that has been studied by others under similar, but primarily photochemical, conditions of 10−50 μM $Co(NO_3)_2$, 100−500 μM $Ru(II)(bpy)_3^{2+}$, 1.0−10.0 mM $Na_2S_2O_8$, hν, and in pH 7.0 or 8.0 sodium phosphate buffer.[36,38,39] That is, if the Co_4POM is actually transformed into a CoO_x catalyst under the reaction conditions, then the

dx.doi.org/10.1021/cs4006925 | ACS Catal. 2014, 4, 79−89

two systems should show similar, if not identical, reaction stoichiometry and kinetics. Alternatively, and as is observed, different stoichiometries and kinetics would be the expected fingerprints of different catalysts.

Controls starting with cobalt(II) nitrate in Table 2 show O_2 yields of 18−56% that decrease with increasing [Ru(III)-

Table 2. O_2 Yields for Ru(III)$(bpy)_3^{3+}$ Plus $Co(NO_3)_2$ Reactions

entry	$[Co(NO_3)_2]$ (μM)	[Ru(III)] (μM)	[Ru(II)] (μM)	pH	O_2 yield (μM)	% yield
1	0.5	500	100	7.2	22	18
2	1.0	500	100	7.2	41	33
3	2.0	500	100	7.2	57	46
4	1	50	100	7.2	7	56
5	1	100	100	7.2	12	48
6	1	200	100	7.2	23	46
7	1	750	100	7.2	52	28
8	1	1000	100	7.2	45	18
9	1	500	50	7.2	39	32
10	1	500	200	7.2	30	24
11	1	500	100	6.8	20	16
12	1	500	100	7.5	42	34
13	1	500	100	7.8	50	40

$(bpy)_3^{3+}$] and that are greater than or equal to those of Co_4POM under identical conditions. The differences between these precursors is even greater when considering that Co_4POM has 4 equiv of cobalt per POM. These results are similar to other studies of cobalt WOCs beginning with cobalt(II) salts or heterogeneous $Co(OH)_2$ colloids because these precedents show higher, up to 90%, selectivity for water oxidation under conditions of pH 9.4 and $[Co(OH)_2]$ = 1 μM and [Ru] = 240−340 μM.[45] Both the prior and current studies of Co^{2+}-derived catalysts indicate the O_2 yield depends on the ratio of oxidant to precatalyst and where the optimal ratio is between 10 and 100.[34,35,46] In contrast, the Co_4POM system shows optimal O_2 yields when >125 equiv of oxidant per cobalt is used (Table 1, entry 6), an observation that distinguishes the reaction stoichiometry when beginning with Co_4POM versus $Co(NO_3)_2$ but does not definitively identify the true catalyst.

Differences between Co_4POM and CoO_x derived from $Co(NO_3)_2$ are also observed in the oxygen evolution kinetics and are the primary evidence for different WOCs in the current study. As seen in Figure 3A, O_2 evolution rates when beginning with $Co(NO_3)_2$ show a first-order dependence on the precatalyst concentration and are 2−11 times faster than identical reactions using Co_4POM. Furthermore, the $\{d[O_2]/dt\}_i$ does not increase significantly with increasing initial $[Ru(III)(bpy)_3^{3+}]$ when 1.0 μM $Co(NO_3)_2$ is used (Figure 3B), which opposes the observed first-order $[Ru(III)(bpy)_3^{3+}]$ dependence when beginning with Co_4POM. This comparison argues that Co^{2+} dissociated from the polyoxometalate core is not forming a significant amount of CoO_x in situ. That is, because the $Co(NO_3)_2$ precatalyst shows first-order and zero-order O_2 evolution kinetic dependencies on the concentration of the precatalyst and $Ru(III)(bpy)_3^{3+}$, respectively, it cannot be the same catalyst as in Co_4POM solutions, which shows first-order dependences on the concentrations of both the precatalyst and $Ru(bpy)_3^{3+}$.

This finding, that CoO_x derived from aqueous Co^{2+} is not the dominant catalyst in the current Co_4POM plus Ru(III)-

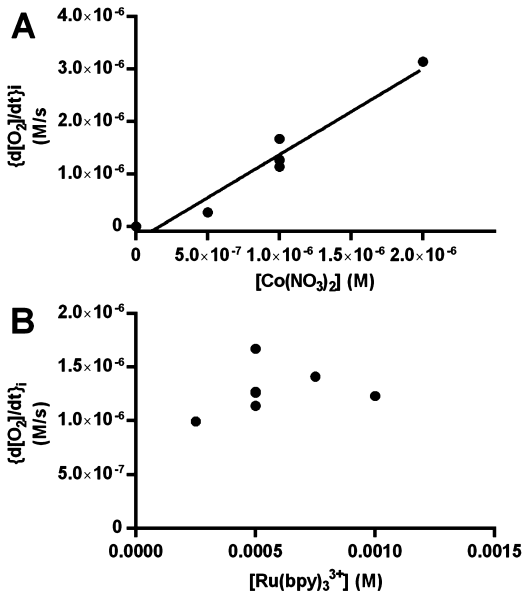

Figure 3. Initial water oxidation rates during controls with variation in the concentrations of the (A) starting $Co(NO_3)_2$ and (B) starting $Ru(III)((bpy)_3^{3+}$. Standard conditions are 1.0 μM $Co(NO_3)_2$, 500 μM $Ru(III)(bpy)_3^{3+}$, 100 μM $Ru(II)(bpy)_3^{2+}$ at pH 7.2 in 0.03 M sodium phosphate buffer. The O_2 was measured using a Clark electrode described in the Experimental Section.[41] The solid line is a linear fit to the initial O_2 evolution rate data.

$(bpy)_3^{3+}$ system, fortifies the investigations of Hill and co-workers[27,28,39] and the observation of Ohlin et al. of enhanced Co_4POM stability in neutral to mildly acidic solutions.[45] Moreover, our prior electrochemical studies,[31] the present study, and those of Hill[39] demonstrate rather clearly that the conditions and, notably, the form of the oxidant can play an important role in determining the kinetically dominant form of WOCs, as we had hinted at in an important footnote (no. 18) in our initial publication in this area.[29] Worth noting here is that our electrochemical oxidation studies employing Co_4POM at higher concentrations (0.5 mM) and pH 8.0 revealed 101 ± 12% of the observed water oxidation catalysis corresponds to CoO_x derived from 58 ± 2 μM Co^{2+} dissociated from the parent polyoxometalate.[29] *The specific conditions, including the oxidant source, do matter in determining the true WOC!*

Investigation of the ligand-oxidation kinetics provides additional insight into the differences between oxidation catalysts derived from $Co(NO_3)_2$ and Co_4POM. As shown in Supporting Information Figure S4, CoO_x shows ligand oxidation rates that are comparable to Co_4POM reactions. This observation of faster water oxidation but comparable ligand oxidation for CoO_x relative to Co_4POM solutions is consistent with the observed higher selectivity for water oxidation for CoO_x vs Co_4POM. Cumulatively, the differences in ligand oxidation and oxygen evolution kinetics strongly support the conclusion herein and elsewhere[27,28,39] that different catalysts are present in the CoO_x and Co_4POM systems when a $Ru(III)(bpy)_3^{3+}$ oxidant is used.

Efforts Toward Constructing a Water Oxidation/Ligand Oxidation Working Mechanistic Hypothesis When Beginning with Co_4POM and $Ru(III)(bpy)_3^{3+}$. In addition to helping distinguish the Co_4POM and $Co(NO_3)_2$ derived catalysts, the kinetics of oxygen evolution and ligand oxidation are invaluable in helping one start to construct a

dx.doi.org/10.1021/cs4006925 | ACS Catal. 2014, 4, 79−89

plausible reaction mechanism, that is, a working mechanistic hypothesis, when starting with Co_4POM and $Ru(III)(bpy)_3^{3+}$. Greatly hindering that effort, however, is that the precise composition of the water-oxidation catalyst has not been fully addressed for the Co_4POM system, either herein or previously,[27,28,39] or, for that matter, for the CoO_x system (although others have examined similar WOCs[34−37,46,47]). Significantly, for the present Co_4POM^{10-} system, neither we nor others know the exact extent and composition of the ion-pairing by $Ru(II)(bpy)_3^{2+}$ and $Ru(III)(bpy)_3^{3+}$ in either the catalytically most active species or in the catalyst resting state.[47] What this means is that any interpretation of the rate law, and especially the *apparent* $[Ru(II)(bpy)_3^{2+}]$ and $[Ru(III)(bpy)_3^{3+}]$ concentration dependencies, needs to be made with caution. And, the presence of a precipitate quantitated herein complicates interpretation of the kinetics even further.

Below, we start our construction of a working mechanistic hypothesis with the assumption that that the catalytically active species is soluble (since that and the presence of a precipitate allowed us to rationalize the observed $\{d[O_2]/dt\}_I$ α $[Co_4POM]^{1\rightarrow 0}$ dependence of the O_2 kinetics, vide supra). Interestingly, and as seen in Figures 1 and 2, the general trends in the oxygen evolution kinetics mirror those seen in the ligand oxidation kinetics and when beginning with Co_4POM. This similarity suggests that the same intermediate(s) is (are) active in both the water oxidation and ligand oxidation reactions; the matching rate trends are also consistent with the constant reaction stoichiometry over a range of initial $Ru(III)(bpy)_3^{3+}$ concentrations.

Combination of the oxygen evolution and ligand oxidation rate data yields the empirical rate law in eq 6.

$$\frac{-d[Ru(III)(bpy)_3^{3+}]}{dt} = (k_1 + k_2)\frac{[Ru(III)(bpy)_3^{3+}][Co_4POM]_{soluble}}{[H^+]} \quad (6)$$

In eq 6, the constants k_1 and k_2 are, then, the apparent rate constants for the parallel paths of O_2 generation and ligand oxidation (and are composite rate constants for the sum of multiple elementary steps). The working hypothesis here is that the amount of catalytically active $[Co_4POM]_{soluble}$ is largely determined by the solubility product equilibrium $[Co_4POM]_{soluble} = \{K_{sp}/[Ru(II)(bpy)_3^{2+}]^3\}^{0.5}$. Although this precipitation equilibrium predicts an inverse 1.5-order in $[Ru(II)(bpy)_3^{2+}]$ if the system is at equilibrium, we observe a roughly inverse first-order dependence (Figures 1B and 2B). This modest difference between predicted and observed rate laws is probably due to the system not actually being at equilibrium; the possibility that the system goes through a 1:1 $Co_4POM/Ru(II)(bpy)_3^{2+}$ complex en route to the equilibrium 2:3 $Co_4POM/Ru(II)(bpy)_3^{2+}$ precipitate is another reason the observed kinetics might look inverse first-order in $[Ru(II)(bpy)_3^{2+}]$. Note that the given rate law is also a simplification because it incorporates the uncatalyzed ligand oxidation reaction rate into k_2; a discussion of this simplification is given in (Supporting Information) eqs S1−S6), which also shows the dependence of $\{-d[Ru(III)(bpy)_3^{3+}]_{ligand\ ox.}/dt\}_i$ on the initial $[Ru(III)(bpy)_3^{3+}]$ in the absence of a catalyst precursor (Supporting Information Figure S5). The rate of oxygen evolution shows a similar empirical rate law, eq 7. A discussion of how this rate law relates to the stoichiometry in eqs 3−5 is given in Supporting Information eqs S7−S9.

$$\frac{d[O_2]}{dt} = \frac{k_1}{4}\frac{[Ru(III)(bpy)_3^{3+}][Co_4POM]_{soluble}}{[H^+]} \quad (7)$$

Because of the complication of precipitation, the precise values of k_1 and k_2 apparent rate constants can only be estimated. Since the observed initial O_2 evolution and $Ru(III)(bpy)_3^{3+}$ loss rates decrease by approximately an order of magnitude when $Ru(II)(bpy)_3^{2+}$ is premixed with the Co_4POM (Supporting Information Figure S2), a zeroth-order approximation is that the $[Co_4POM]$ has also decreased by the same magnitude. That is, using the assumption that the initial $[Co_4POM]$ is 0.1 μM, along with the observed rate law and the slope from Figures 1A and 2A, results in the estimated rate constant values of $k_1 \sim 1.4 \times 10^{-3}$ s^{-1} and $k_2 \sim 4.4 \times 10^{-3}$ s^{-1}.

To check the validity of these constants, the predicted O_2 yield was determined by dividing the O_2 rate constant (k_1) by the sum of the two rate constants ($k_1 + k_2$); a derivation of this calculation is given in Supporting Information eq S7. This calculation results in a predicted O_2 yield of 24%, which is within experimental error of the observed yield of 22% under standard conditions, which is support for at least the consistency, and arguably the validity, of the separately produced experiments, the resultant data, data analyses, and any underlying approximations/assumptions made.

Returning to the construction of a working hypothesis for the proposed WOC mechanism, the resting state of the catalyst at pH 7.2 is most likely $Co^{II}_4(H_2O)_2(PW_9O_{34})_2^{10-}$ (neglecting any ion-pairing to $Ru(II)(bpy)_3^{2+}$ or $Ru(III)(bpy)_3^{3+}$ for the moment) because (i) this species is observed at the end of the reaction by ^{31}P NMR, according to Yin et al.;[27] (ii) the $Ru(bpy)_3^{3+/2+}$ couple occurs at 1.26 V vs NHE, compared with the oxidation wave onset of the Co_4POM solution $E \sim 1.4$ V vs NHE at pH 7.2 (i.e., which implies the majority of the Co_4POM should be in the starting $Co^{II}_4(H_2O)_2(PW_9O_{34})_2^{10-}$ oxidation state);[31] and (iii) Ohlin et al. estimated the pK_a of the Co_4POM to be ~8, and the Co_4POM should therefore have two aquo ligands coordinated to its two outermost cobalts at pH 7.2.[45]

If one interprets the changing $[Co_4POM]^{1\rightarrow 0}$ and the $1/[Ru(II)(bpy)_3^{2+}]$ dependencies in eq 7 in terms of the (demonstrated) precipitate, then one is left with the remaining terms in eq 7 of $d[O_2]/dt$ α $\{[Co_4POM]^1[Ru(III)(bpy)_3^{3+}]^1\}/[H^+]^1$. The simplest interpretation of the remaining terms of that rate law, eq 7, is that a one-electron/one-proton transfer occurs at or before the turnover-limiting step (TLS) of the catalytic cycle (Supporting Information Schemes S1−S2). The observation that the inverse $Ru(II)(bpy)_3^{2+}$ dependence requires premixing of the Co_4POM and $Ru(II)(bpy)_3^{2+}$ suggests the electron-transfer step is not reversible and precipitate formation with the added oxidant $Ru(III)(bpy)_3^{3+}$ is likely not significant within the time needed to take the initial rate measurement (5−10 s). Although consistent with the empirical rate law, this mechanism would require all subsequent (three) electron/proton transfers and O−O bond formation steps to be relatively fast, a requirement that contrasts with the majority of other single-site WOCs in which O−O bond formation is typically turnover-limiting.[14]

Alternatively, it is possible that 2 equiv of $Ru(III)(bpy)_3^{3+}$ reacts with Co_4POM at or prior to the TLS. This hypothetical two-electron transfer would be consistent with the empirical rate law (eq 7) if either (i) the resting state of the catalyst is a $\{[Co_4POM][Ru(III)(bpy)_3^{3+}]\}$ ion pair, which is "on-path" (shown in Scheme 1 and Supporting Information S3), or (ii) a

dx.doi.org/10.1021/cs4006925 | ACS Catal. 2014, 4, 79−89

Scheme 1. One Working Mechanistic Hypothesis for Water Oxidation When Beginning with Co_4POM[a]

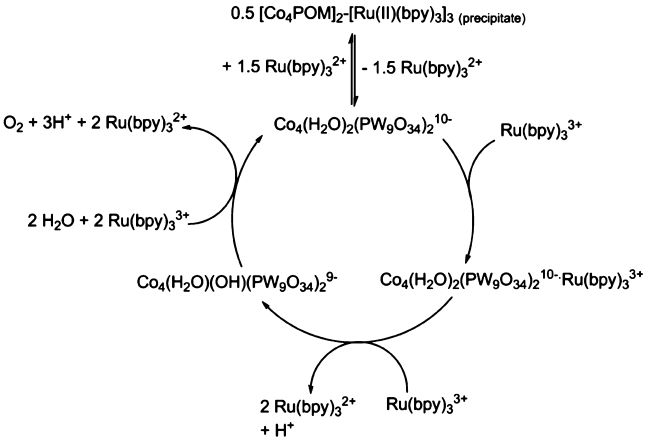

[a] $Co_4(H_2O)_2(PW_9O_{34})_2^{10-}$·$Ru(bpy)_3^{3+}$ is the catalyst resting state in this scheme. Discussion of four detailed mechanisms consistent with the observed kinetics is provided in the Supporting Information for the interested reader.

catalytically inactive {$[Co_4POM][Ru(III)(bpy)_3^{3+}]$} precipitate forms and equilibrates quickly with the solution (Supporting Information Scheme S4). The latter hypothesis, (ii), seems less likely than the former, (i), because the related {$[Co_4POM]_2[Ru(II)(bpy)_3^{2+}]_3$} precipitation reaction appears to be slow compared with the catalyst turnover (vide supra). Therefore, a two-electron/one-proton transfer occurring prior to the TLS is a mechanism that is supported by both prior literature of cobalt WOCs and is consistent with the observed kinetics. Additional discussion and kinetic derivations of possible water oxidation mechanisms are found in the Supporting Information.

However, we note once more that, because of the complications of ion-pairing and precipitation of polyanionioc polyoxoanions, such as Co_4POM^{10-}, with polycations, such as $Ru(II/III)(bpy)_3^{2/3+}$, the mechanism in Scheme 1 is at best an equivocal, working hypothesis. What, however, is unequivocal is that use of polycations such as $Ru(II/III)(bpy)_3^{2/3+}$ as the oxidant with polyanionic precatalysts makes the resultant WOC systems much more complicated, effectively removing many of the reasons for studying, including the intrinsic mechanistic advantages, of such molecular (pre)catalysts.

CONCLUSIONS

Investigation of catalytic water oxidation beginning with $Co_4(H_2O)_2(PW_9O_{34})_2^{10-}$ and $Ru(III)(bpy)_3^{3+}$ has revealed the complexity and nonideal nature of this otherwise interesting, state-of-the-art WOC system. Although Co_4POM is a discrete precatalyst, the use of the $Ru(II/III)(bpy)_3^{2+/3+}$ reagent induces ion-pairing and precipitation of the POM–$Ru(II)(bpy)_3^{2+}$. Oxidative decomposition of the bipyridine ligands is another undesired feature of the system; indeed, O_2 is the minor product in the reaction, corresponding to, at most, a 28% yield under the conditions herein (and based on the initial $[Ru(III)(bpy)_3^{3+}]$). To more efficiently study Co_4POM (and other such) precatalysts, a more robust one-electron oxidant is badly needed,[49] ideally one less highly charged if not neutral or even anionic. As a corollary, it appears the present Co_4POM precatalyst would be a poor choice for incorporation into a photodriven water oxidation system containing organic or organometallic photosensitizers due to the Co_4POM-based catalyst's propensity to oxidize organics relative to the desired substrate, water.

In contrast with the Co_4POM, controls beginning with $Co(NO_3)_2$, which forms heterogeneous CoO_x in situ,[36,38] show a broad range of O_2 yields ranging from 18 to 54%, which are overall higher maximum O_2 yields than Co_4POM (as Hill and co-workers also report[39]). These $Co(NO_3)_2$ controls also show initial O_2 evolution rates that are 2–11 times greater per mol of $Co(NO_3)_2$ than per mol of Co_4POM under otherwise identical conditions, again showing that CoO_x, not Co_4POM, is the superior WOC.

However, although the above data indicate that just 20% of CoO_x could account for the observed water oxidation activity (i.e., ∼0.2 μM CoO_x when starting with 1.0 μM Co_4POM and under the standard conditions herein), the opposing trends in ligand oxidation and differences in the water oxidation rate laws when comparing the $Co(NO_3)_2$ and Co_4POM starting materials argue that CoO_x, at least alone and made from aqueous Co^{2+}, is not the dominant catalyst in this Co_4POM system.

Analysis of the O_2 evolution and $Ru(III)(bpy)_3^{3+}$ reduction initial rates indicates that a one-electron-, one-proton-transfer is involved before the turnover-limiting step in the catalytic cycle, but the ion-pairing and precipitations induced by the $Ru(II/III)(bpy)_3^{2+/3+}$ reagents complicates the system and its kinetics considerably, probably masking the true underlying rate law and turnover-limiting step (Scheme 1, vide supra). However, the kinetic data do indicate that the same reactive intermediate is formed in both the water and ligand-oxidation reactions. This, in turn, means that the selectivity of the catalyst is limited primarily by the catalytic species present and their mechanisms, not by the reaction conditions. This finding has important implications for the limitations of future applications of a Co_4POM-based WOC in artificial photosynthetic schemes: poor selectivity for water oxidation can be anticipated if organics (such as organic photovoltaics or organometallic-based dye-sensitized solar cells) are present.

The present studies issue a caution for comparing TOFs between different systems, and especially between any two systems where the full rate law is not first established for each system. Comparisons of even closely related systems and TOFs on the basis of their "k_{cat}" values could, then, often be an unintended comparison of different mechanisms. Moreover, comparison of different systems on the basis of "k_{obsd}" values is likely to also have an unintended comparison of conditions (i.e., concentration terms in the rate law) in that comparison, as well. This message is timely because of the use and comparison of TOFs is a controversial topic at present.[50−52] Reflection teaches that comparisons of TOFs should be made only after the full rate law for each system being compared is in hand.[51,52]

Overall, the present studies make very apparent that there is a pressing need to find a chemical oxidant other than $Ru(III)(bpy)_3^{3+}$ that is not prone to self-oxidation and that is less highly charged to uncharged for applications with polyanionic precatalysts such as polyometalates. There is also a need for more extensive studies of other Co-POMs to see what are the exceptions, vs the rules, for other Co-POMs as WOCs in comparison with the extant literature of others,[27,28,39] our prior work (i.e., of electrode-bound CoO_x catalysis),[29] and in comparison with the kinetics and implied mechanism uncovered herein. However, kinetics and mechanistic studies at or beyond the present level might best be reserved for other

dx.doi.org/10.1021/cs4006925 | ACS Catal. 2014, 4, 79–89

systems not plagued by precipitation phenomena and in which the primary product of the oxidizing equivalents is the desired O_2.

■ ASSOCIATED CONTENT

Supporting Information

Additional fits and data for $\{d[O_2]/dt\}_i$ and $\{-d[Ru(III)(bpy)_3^{3+}]/dt\}_i$, sample absorbance and oxygen evolution data, K_{sp} measurement data, kinetic controls with both $Co(NO_3)_2$ and no added catalyst, discussion of the uncatalyzed ligand oxidation pathway, and discussion of possible water oxidation mechanisms. This information is available free of charge via the Internet at http://pubs.acs.org/.

■ AUTHOR INFORMATION

Corresponding Author

*E-mail: rfinke@lamar.colostate.edu.

Notes

The authors declare no competing financial interest.

■ ACKNOWLEDGMENTS

J.J.S. thanks the Department of Energy Office of Science for a Graduate Fellowship. This work was supported in part by the Chemical Sciences, Geosciences, and Biosciences Division, Office of Basic Energy Sciences, Office of Science, U.S. Department of Energy, Grant DE-FG02-03ER15453 and the National Science Foundation Grant CHE-0611588. We thank Professor Hill and his colleagues and co-workers for a collegial and cooperative exchange of information, including a preprint of their most recent Co_4POM studies.[39]

■ REFERENCES

(1) Walter, M. G.; Warren, E. L.; McKone, J. R.; Boettcher, S. W.; Mi, Q.; Santori, E. A.; Lewis, N. S. *Chem. Rev.* **2010**, *110*, 6446−6473.
(2) Cook, T. R.; Dogutan, D. K.; Reece, S. Y.; Surendranath, Y.; Teets, T. S.; Nocera, D. G. *Chem. Rev.* **2010**, *110*, 6474−6502.
(3) McDaniel, N. D.; Bernhard, S. *Dalton Trans.* **2010**, *39*, 10021−10030.
(4) Artero, V.; Chavarot-Kerlidou, M.; Fontecave, M. *Ang. Chem. Int. Ed.* **2011**, *50*, 7238−7266.
(5) Tran, P. D.; Artero, V.; Fontecave, M. *Energy Environ. Sci.* **2010**, *3*, 727−747.
(6) Andreiadis, E. S.; Chavarot-Kerlidou, M.; Fontecave, M.; Artero, V. *Photochem. Photobiol.* **2011**, *87*, 946−964.
(7) Herrero, C.; Quaranta, A.; Leibl, W.; Rutherford, A. W.; Aukauloo, A. *Energy Environ. Sci.* **2011**, *4*, 2353−2365.
(8) Gust, D.; Moore, T. A.; Moore, A. L. *Faraday Discuss.* **2012**, *155*, 9−26.
(9) Young, K. J.; Martini, L. A.; Milot, R. L.; Snoeberger, R. C., III; Batista, V. S.; Schmuttenmaer, C. A.; Crabtree, R. H.; Brudvig, G. W. *Coord. Chem. Rev.* **2012**, *256*, 2503−2520.
(10) Du, P.; Eisenberg, R. *Energy Environ. Sci.* **2012**, *5*, 6012−6021.
(11) Swierk, J. R.; Mallouk, T. E. *Chem. Soc. Rev.* **2013**, *42*, 2357−2387.
(12) Liu, X.; Wang, F. *Coord. Chem. Rev.* **2012**, *256*, 1115−1136.
(13) Sartorel, A.; Bonchio, M.; Campagna, S.; Scandola, F. *Chem. Soc. Rev.* **2013**, *42*, 2262−2280.
(14) Wasylenko, D. J.; Palmer, R. D.; Berlinguette, C. P. *Chem. Commun.* **2013**, *49*, 218−227.
(15) Dau, H.; Limberg, C.; Reier, T.; Risch, M.; Roggan, S.; Strasser, P. *ChemCatChem* **2010**, *2*, 724−761.
(16) Finke, R. G.; Droege, M. W. *J. Am. Chem. Soc.* **1984**, *106*, 7274−7277.
(17) Finke, R. G.; Rapko, B.; Saxton, R. J.; Domaille, P. J. *J. Am. Chem. Soc.* **1986**, *108*, 2947−2960.
(18) Geletii, Y. V.; Yin, Q.; Hou, Y.; Huang, Z.; Ma, H.; Song, J.; Besson, C.; Luo, Z.; Cao, R.; O'Halloran, K. P.; Zhu, G.; Zhao, C.; Vickers, J. W.; Ding, Y.; Mohebbi, S.; Kuznetsov, A. E.; Musaev, D. G.; Lian, T.; Hill, C. L. *Isr. J. Chem.* **2011**, *51*, 238−246.
(19) Han, Z. G.; Bond, A. M.; Zhao, C. *Sci. China: Chem.* **2011**, *54*, 1877−1887.
(20) Lv, H.; Geletii, Y. V.; Zhao, C.; Vickers, J. W.; Zhu, G.; Luo, Z.; Song, J.; Lian, T.; Musaev, D. G.; Hill, C. L. *Chem. Soc. Rev.* **2012**, *41*, 7572−7589.
(21) Sartorel, A.; Carraro, M.; Scorrano, G.; Bonchio, M. *Energy Procedia* **2012**, *22*, 78−87.
(22) Murakami, M.; Hong, D.; Suenobu, T.; Yamaguchi, S.; Ogura, T.; Fukuzumi, S. *J. Am. Chem. Soc.* **2011**, *133*, 11605−11613.
(23) Geletii, Y. V.; Besson, C.; Hou, Y.; Yin, Q.; Musaev, D. G.; Quiñonero, D.; Cao, R.; Hardcastle, K. I.; Proust, A.; Kögerler, P.; Hill, C. L. *J. Am. Chem. Soc.* **2009**, *131*, 17360−17370.
(24) Besson, C.; Huang, Z.; Geletii, Y. V.; Lense, S.; Hardcastle, K. I.; Musaev, D. G.; Lian, T.; Proust, A.; Hill, C. L. *Chem. Commun.* **2010**, *46*, 2784−2786.
(25) Sartorel, A.; Miro, P.; Salvadori, E.; Romain, S.; Carraro, M.; Scorrano, G.; Di Valentin, M.; Llobet, A.; Bo, C.; Bonchio, M. *J. Am. Chem. Soc.* **2009**, *131*, 16051−16053.
(26) Natali, M.; Orlandi, M.; Berardi, S.; Campagna, S.; Bonchio, M.; Sartorel, A.; Scandola, F. *Inorg. Chem.* **2012**, *51*, 7324−7331.
(27) Yin, Q.; Tan, J. M.; Besson, C.; Geletii, Y. V.; Musaev, D. G.; Kuznetsov, A. E.; Luo, Z.; Hardcastle, K. I.; Hill, C. L. *Science* **2010**, *328*, 342−345.
(28) Huang, Z.; Luo, Z.; Geletii, Y. V.; Vickers, J. W.; Yin, Q.; Wu, D.; Hou, Y.; Ding, Y.; Song, J.; Musaev, D. G.; Hill, C. L.; Lian, T. *J. Am. Chem. Soc.* **2011**, *133*, 2068−2071.
(29) Stracke, J. J.; Finke, R. G. *J. Am. Chem. Soc.* **2011**, *133*, 14872−14875.
(30) Natali, M.; Berardi, S.; Sartorel, A.; Bonchio, M.; Campagna, S.; Scandola, F. *Chem. Commun.* **2012**, *48*, 8808−8810.
(31) Stracke, J. J.; Finke, R. G. *ACS Catal.* **2013**, *3*, 1209−1219.
(32) Widegren, J. A.; Finke, R. G. *J. Mol. Cat. A: Chem.* **2003**, *198*, 317−341.
(33) Creutz, C.; Sutin, N. *Proc. Nat. Acad. Sci.* **1975**, *72*, 2858−2862.
(34) Brunschwig, B. S.; Chou, M. H.; Creutz, C.; Ghosh, P.; Sutin, N. *J. Am. Chem. Soc.* **1983**, *105*, 4832−4833.
(35) Ghosh, P.; Brunschwig, B. S.; Chou, M.; Creutz, C.; Sutin, N. *J. Am. Chem. Soc.* **1984**, *106*, 4772−4783.
(36) Shevchenko, D.; Anderlund, M. F.; Thapper, A.; Styring, S. *Energy Environ. Sci.* **2011**, *4*, 1284−1287.
(37) Risch, M.; Shevchenko, D.; Anderlund, M. F.; Styring, S.; Heidkamp, J.; Lange, K. M.; Thapper, A.; Zaharieva, I. *Int. J. Hydrogen Energy* **2012**, *37*, 8878−8888.
(38) Hong, D.; Jung, J.; Park, J.; Yamada, Y.; Suenobu, T.; Lee, Y.-M.; Nam, W.; Fukuzumi, S. *Energy Environ. Sci.* **2012**, *5*, 7606−7616.
(39) Vickers, J. W.; Lv, H.; Sumliner, J. M.; Zhu, G.; Luo, Z.; Musaev, D. G.; Geletii, Y. V.; Hill, C. L. *J. Am. Chem. Soc.* **2013**, *135*, 14110−14118.
(40) Weakley, T. J. R.; Evans, H. T.; Showell, J. S.; Tourne, G. F.; Tourne, C. M. *J. Chem. Soc., Chem. Commun.* **1973**, 139−140.
(41) Carano, M.; Holt, K. B.; Bard, A. J. *Anal. Chem.* **2003**, *75*, 5071−5079.
(42) Song, J.; Luo, Z.; Zhu, H.; Huang, Z.; Lian, T.; Kaledin, A. L.; Musaev, D. G.; Lense, S.; Hardcastle, K. I.; Hill, C. L. *Inorg. Chim. Acta* **2010**, *363*, 4381−4386.
(43) Crabtree, R. H. *Chem. Rev.* **2012**, *112*, 1536−1554.
(44) Artero, V.; Fontecave, M. *Chem. Soc. Rev.* **2013**, *42*, 2338−2356.
(45) Ohlin, C. A.; Harley, S. J.; McAlpin, J. G.; Hocking, R. K.; Mercado, B. Q.; Johnson, R. L.; Villa, E. M.; Fidler, M. K.; Olmstead, M. M.; Spiccia, L.; Britt, R. D.; Casey, W. H. *Chem.—Eur. J.* **2011**, *17*, 4408−4417.
(46) Zidki, T.; Zhang, L.; Shafirovich, V.; Lymar, S. V. *J. Am. Chem. Soc.* **2012**, *134*, 14275−14278.
(47) Pestunova, O. P.; Elizarova, G. L.; Parmon, V. N. *Kinet. Catal.* **2000**, *41*, 340−348 and references therein..

(48) (a) Answering the question of the precise composition of the Co_4POM-derived WOC requires knowing the precise speciation of the Co_4POM under the catalytic conditions, that is, any and all forms present in operando.[48b] Then, to determine the true catalyst, the precise, quantitative kinetic contribution of each of those species must be known so that, then, the kinetically dominant form(s) can be determined. (b) Weckhuysen, B. M. *Chem. Commun.* **2002**, 97−110.
(49) A discussion of various oxidants used in water oxidation catalyst testing is given in Parent, A. R.; Crabtree, R. H.; Brudvig, G. W. *Chem. Soc. Rev.* **2013**, *42*, 2247−2252.
(50) Kozuch, S.; Martin, J. M. *ACS Catal.* **2012**, *2*, 2787−2794.
(51) Lente, G. *ACS Catal.* **2013**, *3*, 381−382.
(52) For a classic contribution on the definition and proper use of TOF in catalysis, see: Boudart, M. *Chem. Rev.* **1995**, *95*, 661−666.